

## Radiomics and radiogenomics in pediatric neuro-oncology: A review

Rachel Madhogarhia<sup>†</sup>, Debanjan Haldar<sup>†</sup>, Sina Bagheri, Ariana Familiar, Hannah Anderson, Sherjeel Arif, Arastoo Vossough, Phillip Storm, Adam Resnick, Christos Davatzikos<sup>©</sup>, Anahita Fathi Kazerooni, and Ali Nabavizadeh<sup>©</sup>

*Department of Bioengineering, University of Pennsylvania, Philadelphia, Pennsylvania, USA (R.M.); Center for Biomedical Image Computing and Analytics (CBICA), University of Pennsylvania, Philadelphia, Pennsylvania, USA (R.M., S.A., C.D., A.F.K.); Department of Neurosurgery, Children's Hospital of Philadelphia, Philadelphia, Pennsylvania, USA (D.H., P.S.); Center for Data-Driven Discovery in Biomedicine (D3b), Children's Hospital of Philadelphia, Philadelphia, Pennsylvania, USA (R.M., S.B., A.F., H.A., S.A., A.V., P.S., A.R., A.N.); Institute of Translational Medicine and Therapeutics, Perelman School of Medicine, University of Pennsylvania, Philadelphia, Pennsylvania, USA (D.H.); Department of Radiology, Perelman School of Medicine, University of Pennsylvania, Philadelphia, Pennsylvania, USA (S.B., H.A., S.A., A.V., C.D., A.F.K., A.N.); Department of Radiology, Children's Hospital of Philadelphia, Philadelphia, Pennsylvania, USA (A.V.)*

**Corresponding Author:** Ali Nabavizadeh, MD, Division of Neuroradiology, University of Pennsylvania Health System, 219 Dulles Building, 3400 Spruce Street, Philadelphia, PA 19104, USA ([ali.nabavizadeh@penncmedicine.upenn.edu](mailto:ali.nabavizadeh@penncmedicine.upenn.edu)).

<sup>†</sup>These authors contributed equally to this work.

The current era of advanced computing has allowed for the development and implementation of the field of radiomics. In pediatric neuro-oncology, radiomics has been applied in determination of tumor histology, identification of disseminated disease, prognostication, and molecular classification of tumors (ie, radiogenomics). The field also comes with many challenges, such as limitations in study sample sizes, class imbalance, generalizability of the methods, and data harmonization across imaging centers. The aim of this review paper is twofold: first, to summarize existing literature in radiomics of pediatric neuro-oncology; second, to distill the themes and challenges of the field and discuss future directions in both a clinical and technical context.

### Keywords:

brain tumors | neuro-oncology | pediatrics | radiogenomics | radiomics.

The current era of advanced computing has led to the emergence of the field of radiomics.<sup>1</sup> Radiomics, in brief, is the “high-throughput extraction of large amounts of imaging features” from clinically acquired radiologic images.<sup>2</sup> This data is then compiled into mineable databases and can be utilized in a variety of applications, ranging from hypothesis generation to predictive modeling to clinical decision making.<sup>3</sup> The large-scale impact of the application of this technology becomes clear when one considers the vast amount of underutilized radiologic data generated through routine patient care.<sup>1</sup> Within the field of neuro-oncology, patient tumors are diagnosed and followed through a series of cross-sectional imaging including, but not limited to, CT, MRI, and PET scans. Although each of these scans can contain millions of voxels worth of data, their

analysis is usually limited to qualitative assessments performed by individual neuroradiologists.<sup>1,3</sup> This practice leaves much of the generated data underutilized in the clinical setting and creates a niche that can be filled through the implementation of radiomics.

Radiogenomics, as it is referred to in this review, or imaging genomics, is defined as the integration of radiomics with alterations in molecular and genomic data or using machine learning (ML) methods based on radiomic features to find non-invasive and in vivo signatures to predict molecular alterations in tumors.<sup>4</sup> This technology has shown great potential in the field of neuro-oncology as many disease subtypes have been defined based on their genetic and molecular profiles by the 2021 WHO guidelines.<sup>5</sup> Some theoretical applications of this

technology could allow for the development of noninvasive, “virtual biopsies” which can bridge gaps in histopathological sampling that occur after initial diagnosis when disease progresses or in situations where sophisticated molecular analyses are not readily available.<sup>4</sup>

These technologies have been increasingly applied to a variety of fields and have shown clinical utility in neuro-oncological applications.<sup>6-8</sup> For example, in adult glioma populations, radiomics have been applied to help to characterize molecular subtypes of tumors, differentiate between treatment effects and tumor recurrence,<sup>9</sup> and allow for more accurate survival stratification.<sup>10-13</sup> Furthermore, radiomic profiles of disease could be utilized by clinicians to optimize therapy plans within this group of tumors.<sup>14</sup>

Relative to its adult counterpart, the field of pediatric neuro-oncology has a relative dearth of radiomic studies. The cause of this disparity is unclear and likely multifactorial. One explanation for this could be the simple fact that, among oncological patients, there are far fewer children than adults, and therefore there is less data available upon which to build radiomic models. According to the Central Brain Tumor Registry of the United States (CBTRUS), the incidence rate of brain and other CNS tumors from 2013 to 2017 was about five times higher in adults than in children.<sup>15</sup>

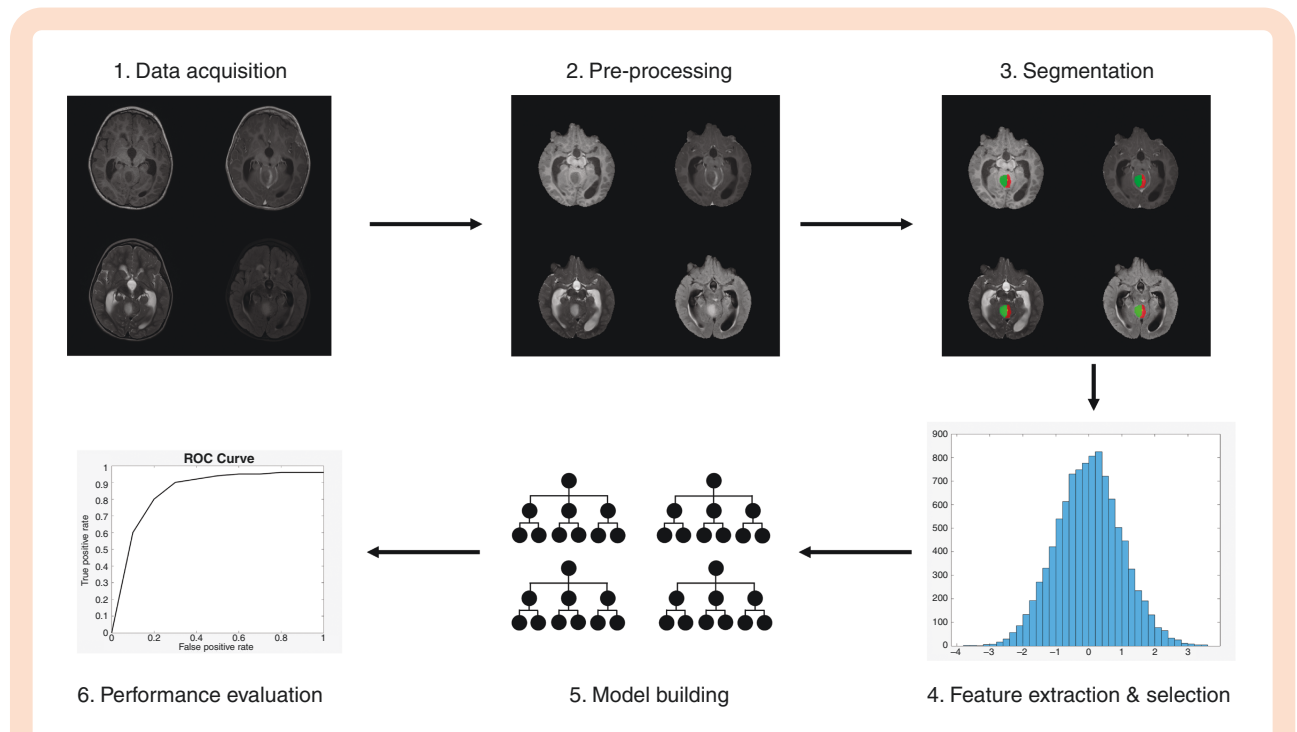
Despite the relative difference in volumes of patients between adult and pediatric populations, childhood brain and other CNS cancers surpass all other cancers as the primary reason for cancer mortality in children.<sup>15</sup> Thus, there is a clear need for further work within these fields.

Figure 1 provides an overview of the workflow commonly used in radiomic studies. We refer the readers interested in learning more about principles of radiomics and radiogenomics studies and their applications to some of the existing excellent review papers on this topic.<sup>1,2,6</sup> The aim of this review paper is twofold: first, to summarize existing literature in radiomics/radiogenomics of pediatric neuro-oncology; second, to distill the themes and challenges of the field and discuss future directions in both a clinical and technical context.

## Pediatric Neuro-Oncology

### WHO Classification of Brain Tumors

For all tumors of the central nervous system, the WHO CNS5 promotes the use of layered and integrated



**Figure 1.** Overview of a typical radiomics workflow. First, the dataset of images and any relevant clinical or genomic data is gathered. Here, T1w, T1wCE, T2w, and FLAIR images are shown. Next, the images are preprocessed through steps such as co-registration and skull stripping. Here, the processed images are shown. Then, tumors are usually segmented by experienced radiologists. Here, the different colors showcase different segmented components on the processed images. Various features are then extracted from each image, usually on the order of hundreds of features per patient. Here, a sample histogram is shown to represent histogram-based features (created in MATLAB). From these features, various models are built, and feature reduction/selection is typically performed to find the most predictive features to prevent overfitting. Random Forest is diagrammed here. Each model built can vary along a few parameters, such as: algorithm (eg, SVM vs RF vs kNN) as well as parameters, feature reduction/selection method, data included (eg, image only vs combined image and clinical data), or image modalities used (eg, T1w vs T2w vs T1w and T2w combined). Finally, each model’s performance is evaluated on a validation and/or external test set based on various metrics such as area under the curve. Here, a sample ROC curve is shown (created in MATLAB).

diagnoses to more comprehensively characterize lesions and capture the depth of information that makes them distinct clinical entities.<sup>5</sup> This layered structure includes an integrated diagnosis, comprised of histopathological classification, CNS WHO grade, and molecular information specific to the subtype. For example, a tumor could have an integrated diagnosis of “Diffuse low-grade glioma, MAPK pathway-altered’ subtype: Diffuse low-grade glioma, *FGFR1 TKD-duplicated*,” a histopathological classification of “Oligodendroglioma,” a CNS WHO grade of “Not assigned,” and molecular information that includes the specific molecular alteration and method of detection.<sup>5</sup> This tiered approach enables precision in both research and clinical settings and highlights the importance of the multimodal approaches to tumor characterization that have been implemented in recent years. It is likely that with advancements in radiomic and radiogenomic fields, features from these modalities will contribute to these layered classification systems, and so by becoming familiar with the current layout, researchers can find opportunities to better differentiate and classify tumors.

## Literature Search Strategy

PubMed and Google Scholar databases were electronically searched to identify relevant studies published prior to May 2021 that included keywords in the title/abstract in the following categories: radiomics (such as “radiomics” or “radiogenomics”), brain tumors (such as “glioma” or “medulloblastoma” or “astrocytoma” or “ependymoma”), and pediatric (such as “pediatric” or “childhood”). Some terms were also searched in medical subject headings, and no limitations were included on the year of publication. Following the initial search, the articles listed in the references of identified studies were evaluated. The search returned 139 articles, 108 of which were excluded after title/abstract review. The remaining articles were reviewed, and studies that met any of the following criteria were excluded: fewer than 75% of patients were pediatric, ML was not used, brain MRI was not the main modality (eg, brain CT only or spine MRI only), no radiomic features were used (ie, studies only using MRS data were excluded), or the tumor was not in the brain (eg, studies on tumors in the spinal cord or elsewhere in the nervous system were excluded). Ultimately, 18 studies were included in the final analysis.

## Summary of Radiomics Studies in Pediatric Neuro-Oncology

In this section, we will review radiomics and radiogenomics studies in pediatric neuro-oncology (summarized in Table 1). We have grouped studies by their endpoint, resulting in four categories: applications in determining tumor histology, applications in identifying disseminated diseases, applications in prognostication, and applications in molecular classification (ie, radiogenomics).

## Applications in Determining Tumor Histology

Determination of tumor histology is a key step in diagnosis and treatment of pediatric brain tumors. Radiomics has shown promise in aiding in the determination of histology even prior to biopsy. This early information can help with surgical planning and better inform caregivers when counseling patients.

**Posterior fossa tumors**—A common goal of radiomic studies in pediatric neuro-oncology has been to distinguish between posterior fossa tumors, particularly Ependymoma (EP), Medulloblastoma (MB), and Pilocytic Astrocytoma (PA)—refer to Table 2 for other abbreviations commonly used throughout this review. These tumors are all located in the posterior fossa, have some similar radiologic characteristics, and patients with these tumors present with similar symptoms. It is clinically important to differentiate between these tumors as this diagnosis can help in guiding surgical or treatment planning, as well as informing prognosis.<sup>34,35</sup> Currently, pathological analysis of the biopsied tissue is the gold standard for diagnosis,<sup>36</sup> but this process is invasive. An accurate radiomic model could allow for a fast, noninvasive method for presurgical and pretreatment diagnosis. Radiomics studies have shown promise in achieving this goal.<sup>16–18,23–26,31,32</sup>

Several of these studies found that classifiers were least accurate in classifying EP. One deep-learning study found that EP had the least distinctive learned feature space amongst these tumors,<sup>26</sup> which may partially explain why posterior fossa classification models often are least accurate at classifying EP among the tumor types. Adding EP patients may help address these difficulties (see Class Imbalance section in the Discussion for further discussion on this topic).

Quantitative information from Diffusion Weighted Imaging (DWI) (Apparent Diffusion Coefficient (ADC) maps) and/or DSC images (unnormalized cerebral blood volume, corrected cerebral blood volume, and/or K2 maps) have been shown to be predictive of classification of posterior fossa tumors.<sup>23,24,31,32</sup> For example, Dong et al. found that several ADC-derived features distinguished EP from MB, which is consistent with the clinical understanding that MB, by virtue of its high cellular density, often restricts diffusion to a greater extent than EP tumors.<sup>32</sup>

In particular, texture-based features derived from T1w and T2w images have been shown to be predictive of posterior fossa tumor classification in both single and multi-institutional studies.<sup>16–18,25</sup>

Most radiomic studies select imaging features from the region of interest drawn around the tumor. However, one study found that imaging features extracted from the whole brain, when combined with imaging features calculated from the region of interest, can improve classification accuracy for posterior fossa tumors.<sup>24</sup> While the mechanism of this improved accuracy is not fully elucidated in the mentioned study, it implies that peri-tumoral regions harbor data that can be meaningful in the clinical context.

**Adamantinomatous craniopharyngioma**—Correct diagnosis of adamantinomatous craniopharyngioma (ACP) is

**Table 1.** Summary of Radiomic Papers from in Pediatric Neuro-Oncology

| Paper                      | Relevant Tumors  | Patient Age Group (Years) | # Subjects and Breakdown, If applicable            | Single or Multi-Institutional (# Centers) | Radiomics Endpoint  | Images Used    | Segmentation Method used | Feature Selection/Reduction Method(s)  | Model(s)  | Performance of Best Model(s), Generally in Terms of AUC  |
|----------------------------|--|---------------------------|--|---|---|----------------|--------------------------|--|---|--|
| Fetit et al. <sup>16</sup> | Pilocytic astrocytoma<br>Medulloblastoma<br>Ependymoma | n/a <sup>a</sup>          | 48 Total<br>breakdown:<br>20 PA<br>21 MB<br>7 EPs  | Single                                    | Differentiate between PA, MB, EP, comparing 2D and 3D texture analysis  | T1w<br>T2w     | Semi-automatic           | Entropy-MDL discretization and PCA   | NB, kNN, classification tree, SVM, ANN, LR  | Best models were LR and ANN on 3D texture features with entropy-MDL-based selection. AUC was 99% (leave-one-out cross-validation and 10-fold cross-validation)   |
| Fetit et al. <sup>17</sup> | Pilocytic astrocytoma<br>Medulloblastoma<br>Ependymoma | n/a                       | 121 Total<br>breakdown:<br>61 PA<br>42 MB<br>18 EP | Multi (3)                                 | Differentiate between PA, MB, EP with 3D texture analysis   | T1w<br>T2w     | Semi-automatic           | Entropy-MDL discretization   | C-SVM   | Overall AUC: 85% (leave-one-out cross-validation)  |
| Fetit et al. <sup>18</sup> | Pilocytic astrocytoma<br>Medulloblastoma<br>Ependymoma | n/a                       | 134 Total<br>breakdown:<br>71 PA<br>45 MB<br>18 EP | multi (3)                                 | Differentiate between PA, MB, EP  | T1w<br>T2w     | Semi-automatic           | Relief, entropy-MDL, and combination of Relief and entropy-MDL   | C-SVM. Included oversampling on EP.   | Mean AUC: 76% (on unseen test set from a different center in pairwise testing). AUC on combined dataset: 86% (before oversampling on EP) and 92% (after oversampling on EP) (leave-one-out cross-validation).  |
| Hara et al. <sup>19</sup>  | Embryonal brain tumors                                 | Median: 6.9               | 34 Total   | Single                                    | Differentiate between various histologies, identify tumors with neuraxis metastases, identify patients at risk of recurrence, and predict survival outcomes from preoperative imaging | T1wCE<br>FLAIR | Manual                   | Selected features that had the largest observed variance within the cohort, and selected ones with physician-defined prognostic value for further analysis | LR to predict sex and M status, multinomial LR for histology, and Cox regression for recurrence and survival outcomes | For histology, key features included size and texture features. For neuraxis metastases, predictive features included tumor diameter (AUC = 0.74) and neighborhood gray tone coarseness (AUC = 0.7). For recurrence, AUC was 0.7 for predictive features such as tumor volume and neighborhood gray tone coarseness. |

**Table 1.** Continued

| Paper                          | Relevant Tumors                  | Patient Age Group (Years)  | # Subjects and Breakdown, If applicable   | Single or Multi-Institutional (# Centers) | Radiomics Endpoint                                      | Images Used                               | Segmentation Method used | Feature Selection/Reduction Method(s)  | Model(s)  | Performance of Best Model(s). Generally in Terms of AUC   |
|--------------------------------|----------------------------------|----------------------------|---|---|---|---|--------------------------|--|---|---|
| Dasgupta et al. <sup>20</sup>  | Medulloblastoma                  | Median: 9<br>range 2–48    | 111 Total<br>Breakdown:<br>17 WNT<br>44 SHH<br>27 Group 3<br>23 Group 4         | Multi (n/a)                               | Predict MB molecular subgroup from preoperative imaging | Multiparametric MRI, including T1wCE, T2w | n/a                      | Pearson chi-square test and Fisher's exact test (on features extracted by observers, such as tumor location, maximum tumor size, and contrast enhancement characteristics, amongst others) | Logistic regression to develop binary nomograms for each subgroup | WNT: AUC of 0.693.<br>SHH: AUC of 0.991.<br>Group 3: AUC of 0.600.<br>Group 4: AUC of 0.788. (validation cohort)  |
| Goya Outi et al. <sup>21</sup> | Diffuse intrinsic pontine glioma | Mean: 7.4                  | 38 Total breakdown:<br>9 H3.1 mutation<br>22 H3.3 mutation<br>4 WT<br>3 unknown | Single                                    | Predict H3 mutation status                              | T1w<br>T2w<br>T1wCE<br>FLAIR              | n/a                      | Multi-level feature selection, including intra-class correlation coefficient, AUC, and hierarchical clustering using spearman's correlation coefficient                                    | SVM, kNN, RF. Included oversampling on minority class (H3.1)      | Best model was SVM with combined imaging and clinical features. This model had F1-weighted score of 0.84 (leave-one-out cross-validation)   |
| Iv et al. <sup>22</sup>        | Medulloblastoma                  | Range: 1 to 18, mean: 8.56 | 109 Total breakdown:<br>30 SHH<br>19 WNT<br>24 Group 3<br>36 Group 4            | Multi (3)                                 | Predict MB molecular subgroup                           | T1wCE<br>T2w                              | Manual                   | Wilcoxon rank sum test   | SVM   | For double 10-fold cross-validation on combined data, best model used both T1wCE and T2w. AUC: 0.79 (SHH), 0.45 (WNT), 0.70 (Group 3), 0.83 (Group 4). T2w-only model had slightly better performance on WNT (0.63).<br>For 3-dataset cross-validation, T1wCE & T2w model had AUC: 0.80 (Group 4), 0.70 (SHH), 0.45 (WNT), 0.39 (Group 3). T1wCE-only model had slightly higher AUC for SHH (0.73). T2w-only model had highest AUC for WNT (0.72) and Group 3 (0.57). |

**Table 1.** Continued

| Paper                      | Relevant Tumors  | Patient Age Group (Years)    | # Subjects and Breakdown, if applicable   | Single or Multi-Institutional (# Centers) | Radiomics Endpoint  | Images Used                                | Segmentation Method Used                                | Feature Selection/Reduction Method(s)   | Model(s)   | Performance of Best Model(s), Generally in Terms of AUC  |
|----------------------------|--|------------------------------|---|---|---|--|---|---|--|--|
| Zhou et al. <sup>23</sup>  | Pilocytic astrocytoma<br>Medulloblastoma<br>Ependymoma                           | Range: 0.25–18, mean: 8.6    | 288 Total<br>breakdown: 107 PA<br>111 MB<br>70 EP                                 | multi (4)                                 | Differentiate between PA, MB, EP  | T1wCE<br>T2w<br>ADC                        | Manual  | Chi-squared score, analysis of variance, T-test, Fisher, Relief, Wilcoxon, mutual information, minimum redundancy/maximum relevance, conditional infomax, joint mutual information, conditional mutual information maximization, interaction capping, double input symmetric relevance, mutual information maximization | Neural network, decision tree, boosting, Bayesian, bagging, RF, SVM, linear discriminant analysis, kNN, generalized linear model. Compared automated optimization of pipeline (with TPOT) with manual expert optimization had AUC: 0.98 (MB), 0.70 (EP), 0.93 (PA) (test set). | Multiclass classification: micro-averaged AUC was 0.91 from TPOT and was 0.92 (chi-squared + generalized linear model) from manual expert optimization (test set). Binary classifiers from TPOT had AUC: 0.94 (MB), 0.84 (EP), 0.94 (PA) (test set). Binary classifiers from manual expert optimization had AUC: 0.98 (MB), 0.70 (EP), 0.93 (PA) (test set). |
| Grist et al. <sup>24</sup> | Pilocytic Astrocytoma<br>Medulloblastoma<br>Ependymoma                           | n/a                          | 49 Total<br>breakdown:<br>22 PA<br>17 MB<br>10 EP                                 | Multi (4)                                 | Differentiate between low-grade (PA) and high-grade (EP, MB), as well as differentiate between PA, MB, and EP | T1w<br>T1wCE<br>T2w<br>FLAIR<br>DWI<br>DSC | n/a   | PCA and UA  | Single layer Neural Network, AdaBoost, RF, SVM, and kNN. Tried oversampling on EP.   | AdaBoost with univariate reduction achieved 85% balanced accuracy (3-fold cross-validation)  |
| Li et al. <sup>25</sup>    | Ependymoma<br>Pilocytic Astrocytoma  | Range: 0–14, mean: 7         | 45 Patients, 135 slices total<br>breakdown: 81 slices EP, 54 slices PA            | Single                                    | Differentiate between EP and PA   | T1w<br>T2w                                 | Manual  | KWT   | SVM  | AUC = 0.88 (validation set)  |
| Quon et al. <sup>26</sup>  | Diffuse midline glioma<br>Medulloblastoma<br>Pilocytic astrocytoma<br>Ependymoma | Range: 0.21–34, median: 6.75 | 617 Total<br>breakdown:<br>122 DMG<br>272 MB<br>135 PA<br>88 EP<br>(+199 control) | Multi (5)                                 | Detection and classification of posterior fossa tumors  | T1wCE<br>T2w<br>ADC                        | Manual (identification of tumor vs. no tumor on slices) | n/a   | Deep-learning architectures (ResNet, ResNeXt, DenseNet, InceptionV3). Used transfer learning. Final prediction made from aggregate slice-level predictions from ensemble of 5 models   | 2D ResNeXt-50-32x4d trained on T2w features had AUC of 0.99 for tumor detection. For classification, accuracy was 92% and F1 was 0.80 (held-out test set). Model's tumor detection accuracy was similar to 4 radiologists; model's classification accuracy and F1 score was higher than 2/4 radiologists   |



Table 1. Continued

| Paper                        | Relevant Tumors                                  | Patient Age Group (Years)    | # Subjects and Breakdown, if applicable   | Single or Multi-Institutional (# Centers) | Radiomics Endpoint   | Images Used                           | Segmentation Method used | Feature Selection/Reduction Method(s)   | Model(s)   | Performance of Best Model(s), Generally in Terms of AUC  |
|------------------------------|--|------------------------------|---|---|--|---------------------------------------|--------------------------|---|--|--|
| Pisapia et al. <sup>27</sup> | Optic pathway gliomas                            | Range: 2–18                  | 38 Total breakdown: 19 with progression 19 without progression  | Single                                    | Predict progression (defined as radiographic tumor growth or vision decline) | T1w T1wCE T2w FLAIR DTI (FA, RAD, TR) | Manual                   | n/a   | SVM  | Model that included features defined as the change in features between pairwise combinations of imaging studies done before progression scan had accuracy: 86% (leave-out-two cross-validation)      |
| Prince et al. <sup>28</sup>  | Adamantinomatous craniopharyngioma               | n/a                          | 39 Total  | Multi (18)                                | Identify ACP   | T1wCT                                 | n/a                      | n/a   | Various pretrained deep-learning neural networks; used transfer learning, genetic algorithm to optimize, and data augmentation | Accuracy of 87.8% for model using features from both MRI and CT, 83.3% for MRI only, and 85.3 for CT only (test set). Model performed on par with average of two human specialists.                  |
| Tam et al. <sup>29</sup>     | Diffuse intrinsic pontine glioma                 | Range: 1.58–19.08 mean: 6.67 | 177 Total   | Multi (11)                                | Prognostication (predict overall survival)                                   | T1wCE T2w                             | Manual                   | Features chosen based on lambda value with minimum cross-validated error across 100 repetitions of 10-fold cross-validation of fitting a Cox regression model | Cox proportional hazards model   | Model using both radiomic and clinical features: concordance was 0.70 (training set) and 0.59 (testing set)  |
| Wagner et al. <sup>30</sup>  | Low-grade gliomas                                | Mean: 9.21                   | 115 Total   | Multi (2)                                 | Predict BRAF molecular status (fusion and V600E point mutation) from imaging | FLAIR                                 | Semi-automatic           | n/a   | RF   | AUC = 0.75 (internal 4-fold cross-validation) and 0.85 (external validation on a cohort from a separate center than training data)   |
| Novak et al. <sup>31</sup>   | Pilocytic astrocytoma Medulloblastoma Ependymoma | Range: 1.0–16.3              | 124 Total breakdown: 36 PA 55 MB 26 EP 7 other (ATRTs + other low-grade tumors not included in classification analysis) | Multi (12)                                | Differentiate between posterior fossa tumors                                 | T1w T2w T1wCE DWI                     | Manual                   | PCA   | NB, RF   | Overall classification accuracy: 86.3% for RF and 84.6% for NB (10-fold cross-validation). NB classified more EP and PA cases correctly than RF, while RF classified more MB cases correctly than NB |

**Table 1.** Continued

| Paper                      | Relevant Tumors               | Patient Age Group (Years) | # Subjects and Breakdown, if applicable   | Single or Multi-Institutional (# Centers) | Radiomics Endpoint            | Images Used               | Segmentation Method used | Feature Selection/Reduction Method(s) | Model(s)                          | Performance of Best Model(s), Generally in Terms of AUC   |
|----------------------------|-------------------------------|---------------------------|---|---|-------------------------------|---------------------------|--------------------------|---------------------------------------|-----------------------------------|---|
| Dong et al. <sup>32</sup>  | Ependymoma<br>Medulloblastoma | Range:<br>0–15            | 51 Total<br>breakdown:<br>24 EP<br>27 MB  | Single                                    | Distinguish between EP and MB | T1wCE<br>DWI              | Semi-automatic           | UA, UAS, MLR                          | kNN, AdaBoost, RF, SVM            | Best model was RF with multivariable logistic regression for feature selection. AUC = 0.91 (10-fold cross-validation)                 |
| Zheng et al. <sup>33</sup> | Medulloblastoma               | Mean: 5.6                 | 124 Total<br>breakdown:<br>44 with CSF dissemination<br>80 without CSF dissemination. | Single                                    | Predict CSF dissemination     | T1w (both head and spine) | Manual                   | mRMR and LASSO                        | Multivariable logistic regression | Best model used combined clinical and radiomic features. AUC: 0.87 (internal validation cohort) and 0.73 (external validation cohort) |

**Abbreviations:** ADC, Apparent Diffusion Coefficient; CSF, Cerebrospinal Fluid; DTI, Diffusion Tensor Imaging; DWI, Diffusion Weighted Imaging; FLAIR, Fluid-attenuated inversion recovery. <sup>a</sup>n/a indicates that the information was not clearly specified (eg, age was not specified for cohort or segmentation methodology was not identified) or the column was not relevant to the particular study (eg, segmentation was not performed).

**Table 2.** Abbreviations

|                                     |                                    |
|-------------------------------------|------------------------------------|
| Brain tumors                        |                                    |
| LGG                                 | Low-Grade Glioma                   |
| HGG                                 | High-Grade Glioma                  |
| PA                                  | Pilocytic Astrocytoma              |
| MB                                  | Medulloblastoma                    |
| EP                                  | Ependymoma                         |
| DIPG                                | Diffuse Intrinsic Pontine Glioma   |
| DMG                                 | Diffuse Midline Glioma             |
| ACP                                 | Adamantinomatous Craniopharyngioma |
| OPG                                 | Optic Pathway Glioma               |
| Classification algorithms           |                                    |
| NB                                  | Naïve Bayes                        |
| RF                                  | Random Forest                      |
| kNN                                 | k-Nearest Neighbors                |
| SVM                                 | Support Vector Machine             |
| C-SVM                               | Cost-Based Support Vector Machine  |
| CNN                                 | Convolutional Neural Network       |
| GBT                                 | Gradient Boosted Trees             |
| LR                                  | Logistic Regression                |
| Feature reduction/selection methods |                                    |
| PCA                                 | Principal Component Analysis       |
| UA                                  | Univariate Analysis                |
| UAS                                 | Univariate Analysis Screening      |
| MLR                                 | Multivariate Logistic Regression   |
| KWT                                 | Kruskal-Wallis Test                |

essential because how ACP is treated and managed differs drastically from other tumors that are considered in the differential diagnosis.<sup>28</sup> For example, germinomas, which are often in the same radiologic differential as ACPs, are effectively treated without surgical intervention whereas ACP often involves aggressive surgical resection and external beam radiation.<sup>28</sup> ACP is accurately diagnosed in 64%–87% of cases.<sup>37</sup> ACP is rare and there is limited available data upon which to build radiomic models. Prince et al. utilized transfer learning, data augmentation, and genetic algorithms to build models from a dataset of 39 patients to identify ACP. They also found that combining CT with MRI scans outperformed either modality alone.<sup>28</sup>

**Embryonal tumors**—Hara et al. found that histological subgroups of embryonal tumors, namely MB, pineoblastoma, and supratentorial primitive neuroectodermal tumors (sPNET), could be differentiated based on texture features as well as quantitative markers of tumor size.<sup>19</sup> Specifically, tumor volume and maximum 3D diameter were associated with specific histologies, with sPNETs being the largest and pineoblastomas being smallest of the three subtypes. This is consistent with clinical reasoning as sPNETs likely go undetected for longer periods of time due to a decreased likelihood of causing hydrocephalus. The study also identified eight textural features that quantified intratumor



heterogeneity that were markedly different between tumor histologies, with pineoblastomas being the most heterogeneous and MBs being the most homogeneous.<sup>19</sup>

### Applications in Identifying Disseminated Disease

The presence of metastasis is important in the staging of many oncologic processes including some primary brain tumors.<sup>38</sup> However, detection of metastatic progression is sometimes difficult and requires a wide array of diagnostic testing some of which can be expensive and invasive. In embryonal tumors, Hara et al. found that radiomic features can discriminate between localized and disseminated disease.<sup>19</sup> Larger primary tumor size was found to be associated with a higher likelihood of neuraxis metastases, and likelihood of neuraxis metastases also trended toward a decrease in primary tumor heterogeneity based on texture features (although these results did not reach statistical significance).<sup>19</sup> In MB patients, Zheng et al. found a clinical-radiomic model to be predictive of preoperative Cerebrospinal Fluid (CSF) dissemination (as determined by head and spine MRI, as well as no subsequent dissemination at the 1-year follow-up for the non-CSF dissemination group).<sup>33</sup>

### Applications in Prognostication

Tumor prognostication, both in terms of survival and risk of recurrence after treatment, is a topic of great interest within the field. While molecular data acquired from biopsy is a current mainstay in tumor classification and prognostication, noninvasive methods that can predict risk of recurrence and overall survival would be hugely beneficial to patients, particularly in cases where biopsy is difficult or unfeasible.

Radiomic features have been shown to be useful in predicting prognosis in optic pathway gliomas (OPGs) and diffuse intrinsic pontine gliomas (DIPGs).<sup>27,29</sup> In developing a model to predict OPG progression, which was defined by radiographic tumor growth and/or vision loss on follow-up scans, Pisapia et al. included data derived from Diffusion Tensor Imaging (DTI), including fractional anisotropy (FA), trace, and radial diffusivity, in addition to features from T1w, T1wCE, T2w, and Fluid-attenuated inversion recovery (FLAIR) sequences.<sup>27</sup> The imaging was acquired as part of a well-defined surveillance protocol. FA features in the optic radiations were found to be among the most predictive features. These results suggest that DTI can measure the changes in the microstructure of white matter that follows tumor growth.<sup>27</sup> For DIPGs, which are progressive and lethal pediatric cancers, intensity-based and texture-based features from wavelet-transformed images have been found to be predictive of overall survival.<sup>29</sup>

In embryonal tumors, larger tumor size and decreased heterogeneity, as measured by their quantitative features, trended toward recurrence of tumors, but these trends did not reach statistical significance based on univariate analyses.<sup>19</sup>

### Radiogenomics for Molecular Classification of Tumors

Radiogenomics, as it is referred to in this review or imaging genomics, is defined as the integration of radiomics

with alterations in molecular and genomic data or using ML methods based on radiomic features to find noninvasive and *in vivo* signatures to predict molecular alterations in tumors.<sup>4</sup> This technology has great promise in the field of neuro-oncology as many disease subtypes have been defined based on their genetic and molecular profiles by WHO guidelines.<sup>5,8</sup>

In pediatrics, models have been developed to predict the molecular subtype of H3 histone mutations in DIPG,<sup>21</sup> molecular subtype in MBs,<sup>20,22</sup> and BRAF mutation.<sup>30</sup>

**H3 molecular subtype in DIPG**—There are two types of H3 mutations frequently associated with diffuse midline gliomas of the pons (generically called DIPG): H3.1K27M and H3.3K27M. A patient's H3 mutation status is clinically important as it guides treatment of DIPG patients and is included in the classification schema of the new WHO CNS5 guidelines.<sup>5</sup>

In one model developed for prediction of H3 mutation subtype among patients with DIPG, three of the six selected imaging features were from FLAIR scans, indicating that the differences in H3 molecular subtype affect some aspect of tumor biology that is reflected in FLAIR scans.<sup>21</sup> This study also found that the combined model of clinical and radiomic features was more accurate than the model built on image data alone.

**MB molecular subtype**—In the recent WHO CNS5 guidelines, MB has been classified into four distinct subgroups based on molecular identity: wingless (WNT)-activated, sonic hedgehog (SHH)-activated and TP53-wildtype, SHH-activated and TP53-mutant, and non-WNT/non-SHH.<sup>5</sup> However, radiogenomic studies have utilized prior guidelines and so discussion of these entities here will have the following identities—WNT, SHH, Group 3, and Group 4 (Groups 3 and 4 are now classified as non-WNT/non-SHH<sup>39</sup>).

Radiomic models generally perform better at predicting SHH and Group 4 than Group 3 and WNT, especially WNT.<sup>20,22</sup> Association has been shown between the presence of peri-tumoral edema, especially moderate to severe edema, and SHH MBs.<sup>20</sup> The location of SHH tumors also has been shown to vary significantly between pediatric patients and adult patients, with them being more commonly located in the midline in the former and lateralized in the latter.<sup>20</sup> One contributing factor to the worse performance of models for prediction of WNT subtype might be that it is the least common subtype of MB, and there were not enough subjects for the predictive models to train on.

lv et al. found that for a dataset that combined data from three institutions into one set, models built from T1wCE and T2w images outperformed models built from either modality alone for all subgroups except WNT. They also explored training models on data from two institutions and testing on the third, and they found that some of the most predictive features that were repeatedly selected in all three loops included features related to lesion area, intensity-based histograms, tumor edge-sharpness, and local area integral invariant.<sup>22</sup>

**BRAF mutations**—Pediatric low-grade gliomas (pLGGs) represent a particularly large and heterogeneous group of tumors where molecular subtyping is a key part of diagnosis and treatment planning. The type of BRAF alteration may play a particularly important role in the prognosis of these tumors. Differentiation between BRAF fusion tumors and BRAF V600E mutated tumors is becoming necessary prior to initiating treatment with certain precision chemotherapeutic agents and has been shown to be important in predicting the clinical course of patients.<sup>40</sup> Wagner et al. developed a model that predicted BRAF status in patients with pLGGs.<sup>30</sup> Features were extracted from FLAIR sequences and included histogram, shape, and texture-based features. Features extracted from 3D wavelet transforms, as well as location of the tumor and patient age at presentation, were especially predictive.

Several of the aforementioned radiogenomic studies that built models on conventional MRI modalities noted that the integration of data from DWI or the resulting ADC maps could improve predictive performances,<sup>20,22,30</sup> but the data were not always routinely available.<sup>20</sup>

## Challenges and Future Directions

There are a number of important challenges that face radiomic studies. In this section, we will discuss these challenges as well as potential solutions and overall trajectory of the field.

### Sample Size

**Small sample size is a widespread challenge**—Many studies had relatively small sample sizes, which most authors noted as a limitation of their models and expressed a desire to increase their patient cohort size in the future. The

sample size of the papers summarized in [Table 1](#) ranged from 34 to 617 brain tumor patients, with a median of 110 patients. One of the reasons contributing to small cohort sizes might be a simple lack of pediatric data. For instance, among oncological patients, there are far fewer children than adults, and therefore there is less data available upon which to build radiomic models specifically for pediatrics compared to adults. In fact, the incidence rate of brain and other CNS tumors from 2013 to 2017 was about five times higher in adults than in children.<sup>15</sup> One group of authors noted that even though EP and MB data have been collected in pediatrics for nearly a decade, their study included a small sample due to the rarity of brain tumors in children overall.<sup>32</sup> Consequences of small sample size include decreased generalizability, increased risk of overfitting, and lack of a separate test cohort.

### Increasing cohort sizes through collaboration and consortia

A long-term solution to small sample size is to use data from multiple institutions through either direct collaboration or utilization of a collective online database. Just under half of the radiomic papers summarized in [Table 1](#) used data from a single institution. Some authors noted that moving forward, multicenter data could be used to increase sample size and evaluate model generalizability.<sup>32,33</sup> There exist a few consortiums to facilitate data collection and sharing,<sup>41,42</sup> such as the Children's Brain Tumor Network, which has several cloud-based platforms, outlined in [Figure 2](#), where researchers can access the data. Other databases relevant for radiomic studies include the National Cancer Institute's Clinical Proteomic Tumor Analysis Consortium (CPTAC) and the Pediatric Brain Tumor Consortium.

One example of how multi-institutional databases can be helpful is the previously discussed study on ACP, which is a rare tumor. The authors used data from the Advancing

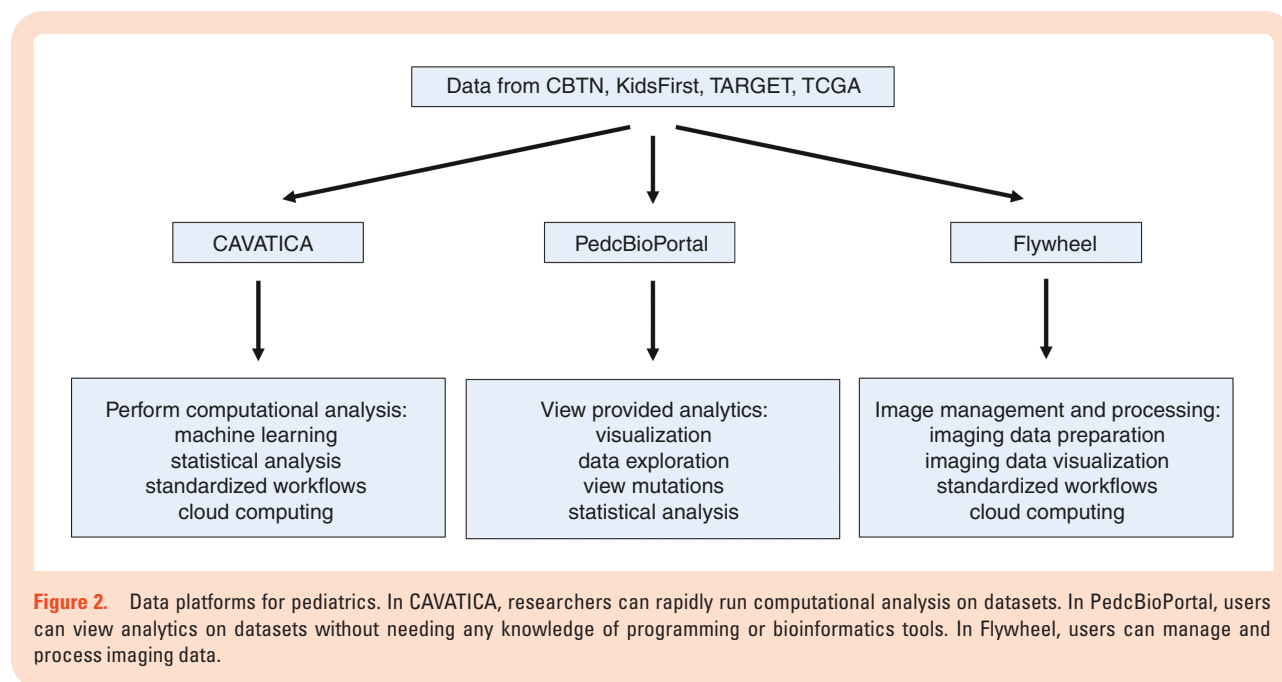


**Figure 2.** Data platforms for pediatrics. In CAVATICA, researchers can rapidly run computational analysis on datasets. In PedcBioPortal, users can view analytics on datasets without needing any knowledge of programming or bioinformatics tools. In Flywheel, users can manage and process imaging data.

Treatment for Pediatric Craniopharyngioma consortium, which provides data from 17 North American centers, along with some data from St. Jude's. This allowed them to build a dataset of 39 patients for a rare brain tumor.<sup>28</sup>

One solution for building such databases is for the radiologists to prospectively capture imaging data and annotate them with a more standardized lexicon.<sup>1</sup> This will help researchers use larger patient cohorts and multicenter data.

Another approach to multi-institutional collaboration is federated learning, which bypasses many of the challenges associated with data sharing.<sup>43,44</sup> In this approach, individual institutions train models on their institutional data. The trained models are then aggregated across institutions into one model. This training process is repeated until a final model is obtained.<sup>44</sup> Recently, federated learning has shown potential for adult brain tumor segmentation from MRI scans.<sup>43</sup>

**Algorithmic solutions to small sample sizes**—A shorter-term solution to having a small data set is to employ transfer learning or data augmentation. Transfer learning allows one to combat the risk of overfitting a model to a small data set by taking an already trained model and using it as the starting point for training on another data set. For example, one study, discussed earlier for work on posterior fossa tumors, used transfer learning from a model that had been pretrained on over 1 million images.<sup>26</sup> Another study used data augmentation, the process of adding synthetic data samples by transforming the original data, in addition to transfer learning.<sup>28</sup> Moving forward, studies with small sample sizes should consider employing these learning techniques to increase the power and generalizability of any findings.

## Class Imbalance

**More studies should explore strategies to mitigate effects of class imbalance**—Many studies summarized in Table 1 faced the challenge of class imbalance, which occurs when the sizes of the classification categories in the training dataset are skewed. In radiomics, class imbalance is often a problem when training a classifier on several cancers where one is rarer than the others, and as a result, there are less samples available for some classes compared to others. To discuss class imbalance, we will use the studies that worked on differentiating between three posterior fossa tumors—MB, PA, and EP—as our example.

PA (and/or sometimes MB) is usually the largest class size, and EP is the smallest. This imbalance makes sense given the tumor incidence rates. According to the CBTRUS age-adjusted incidence rates from 2013 to 2017, in cases per 100,000 persons aged 0 to 19, the incidence rate was 0.92 for PA, 0.40 for MB, and only 0.29 for EP. In fact, PA is the most common brain or CNS tumor in persons aged 0 to 19 years, making up 14.9% of all brain or CNS tumors in pediatrics.<sup>15</sup> The rarity of EP contributes to its disproportionately small class size in radiomic studies, a trend that can be seen in many of the previously discussed studies.<sup>16–18,23,24,31</sup>

Imbalanced multiclass data can be one of the causes of worse performance and lower sensitivity of a classifier on

the minority class (here, EP). One strategy for overcoming class imbalance is balancing the training cohort through undersampling of majority class(es) or oversampling of minority class(es).<sup>45</sup> However, some implementations of these methods, such as random under or oversampling, might reduce the accuracy on the majority class or cause overfitting to the minority class.<sup>45</sup> One study with a training cohort of 71 PA, 45 MB, and 18 EP tumors, created additional synthetic EP samples using the synthetic minority oversampling technique (SMOTE) on the extracted features, which improved their overall classification performance and increased sensitivity of the classifier in discrimination of EP from other posterior fossa tumors. However, it was noted that their generated synthetic samples were included in the leave-one-out cross-validation loops, whereas ideally, performance evaluation would only be based on original samples.<sup>18</sup> Another study outside of those summarized in Table 1 found improved accuracy when combining ensemble learning algorithms with an oversampling technique, SMOTE, for tumor classification from MRS data.<sup>46</sup>

## Multicenter Data and Generalizability

**Multicenter studies to incorporate technological variation**—Using data from multiple centers not only increases sample size, but also aids model generalizability. A problem with radiomic studies is reproducibility.<sup>47</sup> Scanning hardware and scanning protocol differences affect radiomic features to various extents. As such, scanner field strength, manufacturer, family and specific type of MRI sequences, addition of inversion recovery or fat suppression pulses, sequence acquisition parameters, spatial resolution, k-space readout schemes, and scanner image filters might change texture features that are explored in radiomic analyses.<sup>48–52</sup> Several authors discussed previously have noted that incorporating images from various institutions is important because it incorporates a wider range of scanner hardware and protocol differences.<sup>22,30</sup> This variety makes models more robust against these differences, and therefore more generalizable. Although this variety might reduce model accuracy, it is important if a radiomic model is ever to be used beyond a particular set of data.

Several studies have investigated the transferability of radiomic models across institutions with different scanners and/or acquisition protocols by training models on datasets from one or multiple institutions, then testing that model on unseen data from one or multiple different institutions.<sup>18,22</sup> Reported findings indicated that models trained and tested on data combined from all institutions sometimes have slightly higher performance metrics than models trained and tested on data from different institutions, but the latter models still performed well, indicating the potential for successful use of radiomic models across institutions.

**Data harmonization and standardization**—Using multicenter training data presents an additional challenge: data harmonization. Harmonization has been defined as the “explicit removal of site-related effects in multi-site

data.<sup>53</sup> Without harmonization during pre-processing, radiomic models may not be successful when applied to images that were taken with different MRI protocols. Striking a balance between scan protocol variation in the real world and relative harmonization to maximize both accuracy and generalizability is one of the challenges in the field. Several harmonization methods have been developed for MRI, but further research is needed because there is not yet consensus within the radiomics field on what the optimal harmonization method is.<sup>53,54</sup>

The harmonization problem can be mitigated with the standardization of image acquisition protocols. In 2020, the Response Assessment in Pediatric Neuro-Oncology (RAPNO) working group was established to develop recommendations to guide and standardize response assessment in clinical trials for tumor types. Their guidelines on imaging sequences and parameters can also be used in general imaging practices.<sup>55</sup> As more institutions adopt these recommendations, the resulting standardization may make extracted features more reproducible, which should make it easier for radiomic studies to be more generalizable and useful.

#### **Auto-segmentation pipelines to increase generalizability**

Many radiomic studies in the literature have segmented brain tumors from the MRI scans before feature extraction. Full volumetric manual segmentation can be subject to inter-reviewer variability. For example, one study reported that Dice scores between human raters in segmenting sub-regions of gliomas ranged from 74% to 85%.<sup>56</sup> Some studies address this problem by having multiple reviewers delineate tumor regions and reach a consensus about the final segmentation.<sup>29</sup> Inconsistent segmentation guidelines and manual review processes might prohibit the generalizability of radiomic models due to a mismatch in the resulting segmented tumors and their components. In addition, it is time-consuming to segment manually. One potential solution is to develop an automatic segmentation module for pediatric brain cancer, thereby allowing for more consistent segmentations across radiomic studies, a reduction in segmentation time, and easier translation of radiomic models to clinical settings.<sup>57</sup>

Additionally, some studies outside of those in [Table 1](#) used reproducibility or feature stability analysis as a first step in their feature reduction process by removing features that were not reproducible across feature extractions from segmentations performed by different radiologists.<sup>58,59</sup> Future radiomic studies should consider employing similar analyses as this may aid in generalizability of subsequent models.

## **Future Directions**

#### **Combination of multi-omic approaches with radiomics**

While radiomics can provide a plethora of mineable data, their contribution in a clinical context will likely be synergistic with a variety of other systems-based tools. One combination of particular interest is the incorporation of radiomic features with liquid biopsy data for tumor characterization and monitoring of progression. Liquid biopsy refers to the extraction of tumor molecular data from

commonly collected/easily accessible bodily fluids. In practice, cell-free DNA/RNA have shown the most promise and have been used to identify independent prognostic factors in adult pancreatic, lung, and prostate cancer.<sup>60</sup> While neuro-oncology is lagging behind in terms of these advances, there is increasing interest in the use of cell free DNA to characterize and follow primary brain tumors, namely in adult glioblastoma multiforme.<sup>61</sup>

Mutual characteristics (such as noninvasive nature, ease of repeatability, and ease of clinical implementation) of liquid biopsy information and radiomics make them particularly well suited for combination. Over the past several decades, the paradigm of cancer research/treatment has been shifting from static, “one-size” characterization of oncologic entities to granular, dynamical methods. Thus, there is a need for easily implemented and repeatable tests that can more accurately represent the heterogenous and progressive nature of many primary CNS tumors.

**Biological meaning of radiomic features**—In their 2021 paper, Tomaszewski and Gillies emphasized the importance of attaching biological meaning to radiomic findings as the field moves forward.<sup>62</sup> Most studies validate their proposed radiomic signatures using an independent test set. However, biological validation is critical to increase the practical value of these studies and integrate them into clinical decision making. Additionally, providing biological context can help move the field towards acceptance as a standalone method for diagnostics or prognostication. Four classes of biological data that can be correlated to radiomic signatures include: gene expression data, protein expression data from immunohistochemistry, data from local pathologic analysis, and data from habitat imaging. Attaching biological meaning to radiomics can be performed in two ways: either radiomics can be used to predict a biological phenomenon that can then be related to a patient outcome, or the radiomic signature is created to predict a patient outcome and consequently investigated for its association with biologic data.<sup>62</sup>

**Image-localized biopsies**—Given that tumors are often heterogenous and harbor varying genetic and phenotypic aberrations, it is imperative, for the sake of accuracy, that radiogenomic studies correlate imaging findings with the location of biopsy from which molecular information is derived. However, this is seldom the case in retrospective radiogenomic studies. While there has been work done to quantify the spatial uncertainty in radiogenomic models,<sup>63</sup> future endeavors should attempt to co-register image-localized biopsies and imaging pathology. This practice could enable better characterizations of tumors and lead to pipelines that can help guide biopsies to maximize yield of genetic and molecular information.

#### **The future: an open-science platform for clinicians and researchers**

Currently, most radiomic models cannot be used after publication. This is at least in part due to a lack of interoperability and reproducibility, despite the individual models showing potential for helping clinicians in many different ways. Trained radiomic models should be shared



in a centralized platform where they can ultimately be used routinely for clinical applications across institutions. Challenges to this ideal include imaging data storage and management and a lack of standardized file structures and image acquisition protocols across sites. Ongoing efforts to develop systems for data management will help enable efficient workflows across institutions. Software (eg, CaPTk<sup>64</sup>) for processing multimodal data from end-to-end will be essential for widespread implementation of radiomic models.

Finally, multiple expert groups are moving towards standardization of the reporting of radiomic studies, similar to what has been done previously for traditional studies of diagnostic or prognostic performance of imaging exams.<sup>65</sup> This can help improve the quality, repeatability, and reproducibility of radiomic studies and bring them closer to finding clinical applications.

## Conclusion

Radiomics and radiogenomics have been increasingly applied to the field of pediatric neuro-oncology, but many challenges need to be overcome to pave the way for meaningful clinical application. Utilization of multi-institutional databases will be key to the advancement of this field. Despite these unique hurdles, the works reviewed in this article demonstrate the utility of these technologies in aiding in diagnosis, classification, and prognostication of pediatric brain tumors.

## Funding

This work was supported by the National Institutes of Health INCLUDE Supplement—3U2CHL156291-02S1, the Swifty Foundation, and the National Center for Advancing Translational Sciences of the National Institutes of Health (TL1TR001880 to D.H.).

## Acknowledgments

We would like to thank David Higgins for assistance with the database section.

**Conflict of interest statement.** None to declare.

**Authorship statement.** Conceptualization, R.M., D.H., S.B., A.F.K., P.S., C.D., and A.N.; resources, P.S., A.R., C.D., and A.N.; writing—original draft preparation, R.M., D.H., S.B., A.F.K.; writing—review and editing, R.M., D.H., S.B., A.F., H.A., S.A., A.V., P.S., A.R., C.D., A.F.K., and A.N.; supervision, P.S., A.R., C.D., and A.N.; funding acquisition, P.S. and A.R. All authors have read and agreed to the published version of the manuscript.

## References

- Gillies RJ, Kinahan PE, Hricak H. Radiomics: images are more than pictures, they are data. *Radiology* 2016;278(2):563–577.
- Lambin P, Rios-Velazquez E, Leijenaar R, et al. Radiomics: extracting more information from medical images using advanced feature analysis. *Eur J Cancer*. 2012;48(4):441–446.
- Beig N, Bera K, Tiwari P. Introduction to radiomics and radiogenomics in neuro-oncology: implications and challenges. *Neuro-Oncology Advances*. 2020;2(Supplement\_4):iv3–iv14.
- Kazerooni AF, Bakas S, Rad HS, Davatzikos C. Imaging signatures of glioblastoma molecular characteristics: a radiogenomics review. *J Magn Reson Imaging*. 2020;52(1):54–69.
- Louis DN, Perry A, Wesseling P, et al. The 2021 WHO classification of tumors of the central nervous system: a summary. *Neuro-Oncology* 2021;23(8):1231–1251.
- Davatzikos C, Sotiras A, Fan Y, et al. Precision diagnostics based on machine learning-derived imaging signatures. *Magn Reson Imaging*. 2019;64:49–61.
- Kazerooni AF, Davatzikos C. Computational diagnostics of GBM tumors in the era of radiomics and radiogenomics. In: *Lecture Notes in Computer Science (LNCS; Including Subseries Lecture Notes in Artificial Intelligence and Lecture Notes in Bioinformatics)*. Vol 12658 LNCS; 2021.
- Kazerooni AF, Bagley SJ, Akbari H, et al. Applications of radiomics and radiogenomics in high-grade gliomas in the era of precision medicine. *Cancers (Basel)* 2021;13(23):5921.
- Akbari H, Rathore S, Bakas S, et al. Histopathology-validated machine learning radiographic biomarker for noninvasive discrimination between true progression and pseudo-progression in glioblastoma. *Cancer*. 2020;126(11):2625–2636.
- Kazerooni AF, Akbari H, Shukla G, et al. Cancer imaging phenomics via CaPTk: multi-institutional prediction of progression-free survival and pattern of recurrence in glioblastoma. *JCO Clin Cancer Inform*. 2020;4:234–244. doi:10.1200/CCI1900121.
- Macyszyn L, Akbari H, Pisapia JM, et al. Imaging patterns predict patient survival and molecular subtype in glioblastoma via machine learning techniques. *Neuro-Oncology*. 2015;18(3):417–425.
- Kickingeder P, Neuberger U, Bonekamp D, et al. Radiomic subtyping improves disease stratification beyond key molecular, clinical, and standard imaging characteristics in patients with glioblastoma. *Neuro-Oncology*. 2018;20(6):848–857.
- Kickingeder P, Isensee F, Tursunova I, et al. Automated quantitative tumour response assessment of MRI in neuro-oncology with artificial neural networks: a multicentre, retrospective study. *Lancet Oncol*. 2019;20(5):728–740.
- Singh G, Manjila S, Sakla N, et al. Radiomics and radiogenomics in gliomas: a contemporary update. *Br J Cancer*. 2021;125(5):641–657.
- Ostrom QT, Patil N, Cioffi G, et al. CBTRUS statistical report: primary brain and other central nervous system tumors diagnosed in the United States in 2013–2017. *Neuro-Oncology*. 2020;22(suppl 1):iii1–iii105.
- Fetit AE, Novak J, Peet AC, Arvanitis TN. Three-dimensional textural features of conventional MRI improve diagnostic classification of childhood brain tumours. *NMR Biomed*. 2015;28(9):1174–1184.
- Fetit AE, Novak J, Rodriguez D, et al. 3D Texture analysis of heterogeneous MRI data for diagnostic classification of childhood brain tumours. *Stud Health Technol Inform*. 2015;213:19–22.
- Fetit AE, Novak J, Rodriguez D, et al. Radiomics in paediatric neuro-oncology: a multicentre study on MRI texture analysis. *NMR Biomed*. 2018;31(1).

19. Hara JH, Wu A, Villanueva-Meyer JE, et al. Clinical applications of quantitative 3-dimensional MRI analysis for pediatric embryonal brain tumors. *Int J Radiat Oncol Biol Phys.* 2018;102(4):744–756.
20. Dasgupta A, Gupta T, Pungavkar S, et al. Nomograms based on preoperative multiparametric magnetic resonance imaging for prediction of molecular subgrouping in medulloblastoma: results from a radiogenomics study of 111 patients. *Neuro-Oncology.* 2019;21(1):115–124.
21. Goya Outi J, Calmon R, Orhac F, Philippe C, Boddaert N. Can structural MRI radiomics predict DIPG Histone H3 mutation and patient overall survival at diagnosis time? Paper presented at: 2019 IEEE EMBS International Conference on Biomedical & Health Informatics (BHI); May 19–22, 2019; Chicago, IL. 2019:1–4.
22. Lv M, Zhou M, Shpanskaya K, et al. MR imaging-based radiomic signatures of distinct molecular subgroups of medulloblastoma. *Am J Neuroradiol.* 2019;40(1):154–161.
23. Zhou H, Hu R, Tang Q, et al. Automatic machine learning to differentiate pediatric posterior fossa tumors on routine MR imaging. *Am J Neuroradiol.* 2020;41(7):1279–1285.
24. Grist JT, Withey S, MacPherson L, et al. Distinguishing between paediatric brain tumour types using multi-parametric magnetic resonance imaging and machine learning: a multi-site study. *NeuroImage Clin.* 2020;25:102172.
25. Li M, Wang H, Shang Z, et al. Ependymoma and pilocytic astrocytoma: differentiation using radiomics approach based on machine learning. *J Clin Neurosci.* 2020;78:175–180.
26. Quon JL, Bala W, Chen LC, et al. Deep learning for pediatric posterior fossa tumor detection and classification: a multi-institutional study. *Am J Neuroradiol.* 2020;41:1718–1725.
27. Pisapia JM, Akbari H, Rozycki M, et al. Predicting pediatric optic pathway glioma progression using advanced magnetic resonance image analysis and machine learning. *Neuro-Oncol Adv.* 2020;2(1):vdaa090.
28. Prince EW, Whelan R, Mirsky DM, et al. Robust deep learning classification of adamantinomatous craniopharyngioma from limited preoperative radiographic images. *Sci Rep.* 2020;10(1):16885.
29. Tam LT, Yeom KW, Wright JN, et al. MRI-based radiomics for prognosis of pediatric diffuse intrinsic pontine glioma: an international study. *Neuro-Oncol Adv.* 2021;3(1):vdab042.
30. Wagner MW, Hainc N, Khalvati F, et al. Radiomics of pediatric low-grade gliomas: toward a pretherapeutic differentiation of BRAF- mutated and BRAF- fused tumors. *Am J Neuroradiol.* 2021;42(4):759–765.
31. Novak J, Zarinabad N, Rose H, et al. Classification of paediatric brain tumours by diffusion weighted imaging and machine learning. *Sci Rep.* 2021;11(1):2987.
32. Dong J, Li L, Liang S, et al. Differentiation between ependymoma and medulloblastoma in children with radiomics approach. *Acad Radiol.* 2021;28(3):318–327.
33. Zheng H, Li J, Liu H, et al. Clinical-MRI radiomics enables the prediction of preoperative cerebral spinal fluid dissemination in children with medulloblastoma. *World J Surg Oncol.* 2021;19(1):134.
34. Muzumdar D, Ventureyra EC. Treatment of posterior fossa tumors in children. *Expert Rev Neurother.* 2010;10(4):525–546.
35. Poretti A, Meoded A, Huisman TAGM. Neuroimaging of pediatric posterior fossa tumors including review of the literature. *J Magn Reson Imaging.* 2012;35(1):32–47.
36. Huttner A. Overview of primary brain tumors: pathologic classification, epidemiology, molecular biology, and prognostic markers. *Hematol Oncol Clin North Am.* 2012;26(4):715–732.
37. Norris GA, Garcia J, Hankinson TC, et al. Diagnostic accuracy of neuroimaging in pediatric optic chiasm/sellar/suprasellar tumors. *Pediatr Blood Cancer.* 2019;66(6):e27680.
38. Chang CH, Housepian EM, Herbert C. An operative staging system and a megavoltage radiotherapeutic technic for cerebellar medulloblastomas. *Radiology* 1969;93(6):1351–1359.
39. Taylor MD, Northcott PA, Korshunov A, et al. Molecular subgroups of medulloblastoma: the current consensus. *Acta Neuropathol.* 2012;123(4):465–472.
40. Lassaletta A, Zapotocky M, Mistry M, et al. Therapeutic and Prognostic Implications of BRAF V600E in Pediatric Low-Grade Gliomas. *J Clin Oncol.* 2017;35(25):2934.
41. *First Large-scale, Multicenter Proteogenomic Analysis Offers New Insights into Pediatric Brain Tumor Biology.* Bethesda, MD: National Cancer Institute. [https://proteomics.cancer.gov/news\\_and\\_announcements/first-large-scale-multicenter-proteogenomic-analysis-offers-new-insights](https://proteomics.cancer.gov/news_and_announcements/first-large-scale-multicenter-proteogenomic-analysis-offers-new-insights). Accessed February 5, 2022.
42. Pediatric Brain Tumor Consortium. <https://www.pbtc.org>. Accessed November 24, 2021.
43. Sheller MJ, Edwards B, Reina GA, et al. Federated learning in medicine: facilitating multi-institutional collaborations without sharing patient data. *Sci Rep.* 2020;10(1):12598.
44. Rieke N, Hancox J, Li W, et al. The future of digital health with federated learning. *npj Digital Med.* 2020;3(1):119.
45. Shuo W, Xin Y. Multiclass imbalance problems: analysis and potential solutions. *IEEE Trans Syst Man Cybern B.* 2012;42(4):1119–1130.
46. Zarinabad N, Wilson M, Gill SK, et al. Multiclass imbalance learning: improving classification of pediatric brain tumors from magnetic resonance spectroscopy. *Magn Reson Med.* 2017;77(6):2114–2124.
47. Traverso A, Wee L, Dekker A, Gillies R. Repeatability and reproducibility of radiomic features: a systematic review. *Int J Radiat Oncol Biol Phys.* 2018;102(4):1143–1158.
48. Ford J, Dogan N, Young L, Yang F. Quantitative radiomics: impact of pulse sequence parameter selection on MRI-Based textural features of the brain. *Contrast Media Mol Imaging.* 2018;2018:1729071.
49. Yang F, Dogan N, Stoyanova R, Ford JC. Evaluation of radiomic texture feature error due to MRI acquisition and reconstruction: a simulation study utilizing ground truth. *Phys Medica.* 2018;50:26–36.
50. Mayerhoefer ME, Szomolanyi P, Jirak D, Materka A, Trattnig S. Effects of MRI acquisition parameter variations and protocol heterogeneity on the results of texture analysis and pattern discrimination: an application-oriented study. *Med Phys.* 2009;36(4):1236–1243.
51. Savio SJ, Harrison LC, Luukkaala T, et al. Effect of slice thickness on brain magnetic resonance image texture analysis. *Biomed Eng Online.* 2010;9(1):60.
52. Waugh SA, Lerski RA, Bidaut L, Thompson AM. The influence of field strength and different clinical breast MRI protocols on the outcome of texture analysis using foam phantoms. *Med Phys.* 2011;38(9):5058–5066.
53. Pomponio R, Erus G, Habes M, et al. Harmonization of large MRI datasets for the analysis of brain imaging patterns throughout the lifespan. *Neuroimage.* 2020;208:116450.
54. Carré A, Klausner G, Edjlali M, et al. Standardization of brain MR images across machines and protocols: bridging the gap for MRI-based radiomics. *Sci Rep.* 2020;10(1).
55. Erker C, Tamrazi B, Poussaint TY, et al. Response assessment in paediatric high-grade glioma: recommendations from the Response Assessment in Pediatric Neuro-Oncology (RAPNO) working group. *Lancet Oncol.* 2020;21(6):e317–e329.
56. Menze BH, Jakab A, Bauer S, et al. The multimodal brain tumor image segmentation benchmark (BRATS). *IEEE Trans Med Imaging.* 2015;34(10):1993–2024.
57. Madhogarhia R, Fathi Kazerooni A, Arif S, et al. Automated segmentation of pediatric brain tumors based on multi-parametric MRI and deep learning. In: Iftekharruddin KM, Drukker K, Mazurowski MA,



- Lu H, Muramatsu C, Samala RK, eds. *Proc. SPIE 12033, Medical Imaging 2022: Computer-Aided Diagnosis; April 4, 2022; San Diego, CA; 2022:124.*
58. Kandemirli SG, Kocak B, Naganawa S, et al. Machine learning-based multiparametric magnetic resonance imaging radiomics for prediction of H3K27M mutation in midline Gliomas. *World Neurosurg.* 2021;151:e78–e85.
  59. Dong F, Li Q, Xu D, et al. Differentiation between pilocytic astrocytoma and glioblastoma: a decision tree model using contrast-enhanced magnetic resonance imaging-derived quantitative radiomic features. *Eur Radiol.* 2019;29(8):3968–3975.
  60. Wang J, Chang S, Li G, Sun Y. Application of liquid biopsy in precision medicine: opportunities and challenges. *Front of Med.* 2017;11(4):522–527.
  61. Yekula A, Muralidharan K, Rosh Z, et al. Liquid biopsy strategies to distinguish progression from pseudoprogression and radiation necrosis in Glioblastomas. *Adv Biosyst.* 2020;4(12):e2000029.
  62. Tomaszewski MR, Gillies RJ. The biological meaning of radiomic features. *Radiology* 2021;299(2):E256–E256.
  63. Hu LS, Wang L, Hawkins-Daarud A, et al. Uncertainty quantification in the radiogenomics modeling of EGFR amplification in glioblastoma. *Sci Rep.* 2021;11(1).
  64. Davatzikos C, Rathore S, Bakas S, et al. Cancer imaging phenomics toolkit: quantitative imaging analytics for precision diagnostics and predictive modeling of clinical outcome. *J Med Imaging.* 2018;5(01):1.
  65. Pfaehler E, Zhovannik I, Wei L, et al. A systematic review and quality of reporting checklist for repeatability and reproducibility of radiomic features. *Physics and Imaging in Radiation Oncology* 2021;20:69–75.